

Dynamics of clathrin and adaptor proteins during endocytosis

Joshua Z. Rappoport, Shahrnaz Kemal, Alexandre Benmerah and Sanford M. Simon

Am J Physiol Cell Physiol 291:C1072-C1081, 2006. doi:10.1152/ajpcell.00160.2006

You might find this additional info useful...

Supplemental material for this article can be found at:

<http://ajpcell.physiology.org/content/suppl/2007/01/05/291.5.C1072.DC1.html>

This article cites 46 articles, 24 of which can be accessed free at:

<http://ajpcell.physiology.org/content/291/5/C1072.full.html#ref-list-1>

This article has been cited by 2 other HighWire hosted articles

Imaging with total internal reflection fluorescence microscopy for the cell biologist

Alexa L. Mattheyses, Sanford M. Simon and Joshua Z. Rappoport

J Cell Sci, October, 21 2010; 123 (21): 3621-3628.

[Abstract] [Full Text] [PDF]

Regulation of Hip1r by epsin controls the temporal and spatial coupling of actin filaments to clathrin-coated pits

Rebecca J. Brady, Cynthia K. Damer, John E. Heuser and Theresa J. O'Halloran

J Cell Sci, October, 21 2010; 123 (21): 3652-3661.

[Abstract] [Full Text] [PDF]

Updated information and services including high resolution figures, can be found at:

<http://ajpcell.physiology.org/content/291/5/C1072.full.html>

Additional material and information about *AJP - Cell Physiology* can be found at:

<http://www.the-aps.org/publications/ajpcell>

This information is current as of March 22, 2011.

Dynamics of clathrin and adaptor proteins during endocytosis

Joshua Z. Rappoport,¹ Shahrnaz Kemal,¹ Alexandre Benmerah,² and Sanford M. Simon¹

¹Laboratory of Cellular Biophysics, Rockefeller University, New York, New York; and ²Department of Infectious Diseases, Institut Cochin, Institut National de la Santé et de la Recherche Médicale U567, Centre National de la Recherche Scientifique Unité Mixte de Recherche 8104, Université Paris 5, Paris, France

Submitted 6 April 2006; accepted in final form 26 May 2006

Rappoport, Joshua Z., Shahrnaz Kemal, Alexandre Benmerah, and Sanford M. Simon. Dynamics of clathrin and adaptor proteins during endocytosis. *Am J Physiol Cell Physiol* 291: C1072–C1081, 2006. doi:10.1152/ajpcell.00160.2006.—The endocytic adaptor complex AP-2 colocalizes with the majority of clathrin-positive spots at the cell surface. However, we previously observed that AP-2 is excluded from internalizing clathrin-coated vesicles (CCVs). The present studies quantitatively demonstrate that AP-2 disengages from sites of endocytosis seconds before internalization of the nascent CCV. In contrast, epsin, an alternate adaptor for clathrin at the plasma membrane, disappeared, along with clathrin. This suggests that epsin remains an integral part of the CCV throughout endocytosis. Clathrin spots at the cell surface represent a heterogeneous population: a majority (70%) of the spots disappeared with a time course of 4 min, whereas a minority (22%) remained static for ≥ 30 min. The static clathrin spots undergo constant subunit exchange, suggesting that although they are static structures, these spots comprise functional clathrin molecules, rather than dead-end aggregates. These results support a model where AP-2 serves a cargo-sorting function before endocytosis, whereas alternate adaptors, such as epsin, actually link cargo to the clathrin coat surrounding nascent endocytic vesicles. These data also support a role for static clathrin, providing a nucleation site for endocytosis.

adaptor complex; epsin; total internal reflection fluorescence microscopy

CLATHRIN-MEDIATED ENDOCYTOSIS is responsible for the internalization of cargo ranging from nutrients to viruses. This process is evolutionarily conserved among eukaryotes (8, 11, 36). Biochemical assays and in vitro analyses have characterized many details in the assembly of the cytoplasmic clathrin coats to result in clathrin-coated pits (CCPs), pit invagination, and fission of a clathrin-coated vesicle (CCV). This process, organized around three main players, clathrin, the heterotetrameric adaptor complex AP-2, and the GTPase dynamin, has been described in detail in several recently published reviews (19, 37, 40). In this model, the AP-2 complex plays a central role in CCP assembly and function: it is responsible for the assembly of clathrin triskelia on the cytosolic leaflet of the plasma membrane and the selection of cargo to be internalized.

Clathrin-associated proteins are generally separated into two categories: adaptors, such as AP-2, which bind cargo, and accessory proteins, which facilitate endocytosis. Epsin, clathrin assembly lymphoid myeloid leukemia (CALM), AP180, Hip1, Hip1 related, numb, Dab2, Arh, and β -arrestins are classified as “alternate adaptors” (i.e., alternate to AP-2) because of their ability to bind clathrin and cargo (41). Furthermore, epsin, Eps-15, and CALM/AP180 seem to be involved in recruitment of AP-2 onto the plasma membrane (3, 4, 13, 20). Another role

ascribed to epsin is that of inducing membrane curvature in lipid bilayers and, therefore, driving the curvature of clathrin coats in vitro (12). These findings have suggested that epsin may play a crucial role in the invagination process, resulting in classification of epsin as an adaptor and an accessory protein (43).

The efforts to categorize proteins into distinct functional classes have resulted in a number of unresolved, and apparently contradictory, observations. One such issue is whether epsin represents a peripheral endocytic factor or remains associated with nascent vesicles subsequent to fission from the plasma membrane. Some biochemical data and several review articles have suggested that epsin has a role only before internalization of CCVs (7, 28, 29). However, a more recent study employing tandem mass spectroscopy and immunoblotting has provided evidence that epsin is specifically retained within a CCV fraction (6). The seemingly contradictory results produced from similar techniques call for the application of an alternate methodology for evaluation of this issue. Furthermore, although AP-2 is the adaptor most frequently associated with endocytosis, AP-2 is not found in the clathrin spots that are internalizing from the membrane surface (30, 33).

One key to resolving these potential discrepancies comes from the observation that clathrin exists as a heterogeneous population at the cell surface. Observations of clathrin dynamics over the course of 1 min indicate the existence of three distinct populations in association with the plasma membrane: static CCPs (80%), disappearing CCVs (15%), and laterally mobile spots (5%) (31, 34). Biochemical observations, by their nature, average all the interactions in the cell. However, with imaging, it is possible to discriminate the activity of a multitude of subpopulations, even minority populations, and the dynamics of their behavior.

One imaging modality that is particularly appropriate for studying endocytosis is total internal reflection fluorescence microscopy (TIR-FM), which selectively illuminates only fluorophores at the cell surface (1). Application of live-cell dual-color TIR-FM to the study of endocytosis has provided some data that match the expected results: cargo such as transferrin (Tf) and transferrin receptor (TfR) disappear along with clathrin (26, 30), and dynamin-1 rapidly increases in intensity immediately before the disappearance of clathrin (25, 33, 39). Other findings were unexpected, such as the report that disappearing clathrin spots (CCVs) are generally devoid of the AP-2 complex relative to static spots (CCPs) (33). These results suggest a new model for CCP/CCV formation, in which the AP-2 complex is excluded from forming CCVs and may

Address for reprint requests and other correspondence: S. M. Simon, Laboratory of Cellular Biophysics, Rockefeller Univ., 1230 York Ave., Box 304, New York, NY 10021 (e-mail: simon@rockefeller.edu).

The costs of publication of this article were defrayed in part by the payment of page charges. The article must therefore be hereby marked “advertisement” in accordance with 18 U.S.C. Section 1734 solely to indicate this fact.

form platforms for cargo selection from which vesicles may form. They also raise many issues, such as the origin of the AP-2-negative and clathrin-positive disappearing spots and also the putative adaptor for clathrin in these internalizing structures.

The present analysis addresses these issues. To specifically evaluate whether the endocytic clathrin puncta originate from sites in which clathrin and AP-2 colocalize or whether they are completely independent, we followed the dynamics of clathrin for long (5- to 30-min) periods, instead of ~ 1 min, as in our previous studies. In this way, we were able to demonstrate that AP-2 can disengage from sites of endocytosis seconds before internalization of the nascent CCV. Finally, the observation that epsin remains colocalized with clathrin during the entire period of internalization suggests that another level of heterogeneity exists: not all endocytic adaptors have similar dynamics during endocytosis. These results demonstrate some advantages of studying single events, particularly when a heterogeneous population is examined.

To further evaluate the static population of clathrin, we observed cells continuously for longer time periods in this study than in previous studies and documented that 22% of clathrin spots remain in place for ≥ 30 min. Finally, we evaluated whether static clathrin puncta that remain on the cell surface for extended periods of time are functional in terms of subunit exchange with cytosolic clathrin. Active subunit exchange has been shown to be necessary in the transition from CCPs to CCVs, and in the event that endocytosis is blocked by potassium depletion or hypertonic sucrose, clathrin exchange is inhibited (24, 44, 45). Analysis of static clathrin spots by fluorescence recovery after photobleaching (FRAP) demonstrated that clathrin exchange occurs in this population and suggested that static clathrin spots might play an active role in the process of endocytosis, potentially as sorting centers from which cargo-laden nascent CCVs can bud.

MATERIALS AND METHODS

Plasmid constructs and cell culture. The preparation and use of all constructs have been previously described. HeLa cells were maintained in DMEM with 10% FBS in a 37°C incubator humidified with 5% CO₂ and imaged ~ 48 h after transfection with FuGene6 (Roche Diagnostics, Indianapolis, IN) for TIR-FM or a calcium phosphate kit (Invitrogen, Carlsbad, CA) for immunocytochemistry studies.

TIR-FM image acquisition. TIR-FM was performed at 37°C, as previously described (30–34, 38), using the Apo $\times 60$ 1.45 NA microscope objective (Olympus America, Melville, NY). Previous studies indicate that excitation decreases to $1/e$ in < 100 nm with this TIR-FM configuration (22). DsRed-labeled clathrin (clathrin-DsRed) and enhanced green fluorescent protein (EGFP)-labeled α -adaptin (or epsin-EGFP) were excited with the 488-nm line of a tunable argon laser (Omnichrome, model 543-AP A01, Melles Griot, Carlsbad, CA) reflected off a 498-nm dichroic mirror. All mirrors and filters were obtained from Chroma Technologies (Branford, VT). Green and red emissions were collected simultaneously using a dual-view splitter (Optical Insights, Santa Fe, NM) equipped with a 515/30-nm band-pass filter to collect green emission, a 550-nm dichroic mirror to split the emission, and a 580-nm long-pass filter to collect red emission. Clathrin-DsRed imaging was performed with the 514-nm line of the same tunable argon laser reflected off a polychroic mirror (442/514 pc), and emitted light was collected through a 580-nm long-pass filter.

All time-lapse studies were carried out with exposure times of 100 ms per frame and total illumination limited to 30 or 60 s. Images were obtained every 500 ms for 5 min (clathrin-DsRed and EGFP- α -

adaptin), every 1 s for 10 min (clathrin-DsRed), or every 6 s for 30 min (clathrin-DsRed). For continuous-illumination studies (clathrin-DsRed and epsin-EGFP), streams of 100–300 frames were acquired at 100–300 ms per frame for a total acquisition time of ~ 30 s.

Dual-color processing. For simultaneous dual-channel imaging, after subtraction of extracellular background, 12-bit dual-color TIR-FM image streams were aligned using a journal written for MetaMorph (Universal Imaging, Downingtown, PA) (30). On the basis of preliminary single-fluorophore control experiments, green-to-red bleed-through corrections of 10% for EGFP- α -adaptin (or epsin-EGFP) and clathrin-DsRed were employed (30); after alignment, 10% of the EGFP signal was subtracted from the DsRed images.

FRAP studies. Static EGFP-clathrin spots were identified by analysis of 10-min time lapses of 50-ms exposures collected every 2 s. A circular (~ 15 - μ m-diameter) region was bleached for 60 s by closing an iris in front of the TIR-FM laser. Immediately after photobleaching, a second time lapse was acquired for 10 min with 100-ms exposures collected every 15 s. During image analysis, static spots were identified from within the bleached region from the prebleach time lapse, and a total of 89 static spots from 3 cells were evaluated for fluorescence recovery after photobleaching. The time taken for each of the 89 spots to reach one-half of maximum fluorescence intensity ($t_{1/2}$) during the 10-min recovery period was calculated and averaged.

Analysis of time-lapse data sets. For the analysis of clathrin-DsRed at the sites of EGFP- α -adaptin disappearance, a total of 89 spots from 4 time-lapse data sets (100 ms acquired every 500 ms for 5 min) were evaluated. The location and time of EGFP- α -adaptin disappearance were identified, and the corresponding region in the clathrin-DsRed channel was evaluated. Spots were identified as disappearing if the fluorescence dropped to background (and did not change for multiple frames) and as mobile if they moved laterally for more than one spot diameter over the course of a few frames. Mobile spots, spots that moved laterally and subsequently fused with another spot, and spots that remained at the end of the time-lapse data set were categorized as “did not disappear.” The result of the analysis of each of the 89 identified spots was evaluated with a histogram.

To determine the proportion of static clathrin-DsRed spots remaining 10, 20, and 30 min after the start of imaging (100 ms acquired every 6 s for 30 min), 200 spots per time lapse (5 time lapses total) were circled in the first frame with a region-marking tool in MetaMorph. Clathrin spots were identified as static if they did not move laterally relative to any general cell drift or if they did not move into the cell during the entire length of the acquired time lapse. Each selected spot was tracked throughout the time lapse to account for local motion (of spots and cells); the entire data set (300 frames, 30 min) was subdivided into three 10-min subsets that were each analyzed sequentially. Thus the 200 spots identified at *time 0* were tracked for 10 min, and each of the remaining spots was identified in the next set (10–20 min) by transfer of each of the remaining regions. The same procedure was followed at 20 min. The total number of spots that remained at each time point was averaged and plotted as a mean percentage.

Immunocytochemistry studies. Immunocytochemistry was used to study epsin-EGFP-transfected cells, as previously described (2, 33). Primary antibodies included mouse monoclonal anti-human TfR (CD71) from Sigma and rabbit polyclonal anti- α -adaptin (M300), goat polyclonal anti-CALM (C-18), and anti-Eps-15 (K-15) from Santa Cruz Biotechnology (Santa Cruz, CA). Anti-clathrin was derived from the CON.1 hybridoma (American Type Culture Collection, Manassas, VA), and anti-Eps-15 (3T) was a gift from Dr. Pier Di Fiore (European Institute of Oncology, Milan, Italy). Alexa Fluor 594-labeled goat anti-mouse, goat anti-rabbit, and donkey anti-goat immunoglobulins were purchased from Molecular Probes (Invitrogen). Samples were viewed under an epifluorescence microscope (Leica) with a cooled charge-coupled device camera (Micromax, Princeton Instruments). Images were acquired using MetaMorph and

processed with MetaMorph, NIH Image (<http://rsb.info.nih.gov/ni-image/>), and Photoshop (Adobe Systems, San Jose, CA).

Tf uptake. At 48 h after transfection, cells transfected with EGFP, epsin-EGFP, or AP180c-EGFP in six-well plates (2 wells per construct) were rinsed with warm PBS and placed in warm serum-free medium for 30 min in a 37°C incubator to chase out cell surface-bound Tf. The cells were incubated for 30 min in a 37°C incubator in Alexa Fluor 633-labeled Tf (Molecular Probes) diluted 1:100 in serum-free medium from a 5 mg/ml stock (50 µg/ml final concentration), rinsed in PBS, and placed in DMEM with 10% FBS for 5 min at 37°C. Finally, the cells were rinsed in PBS, detached by incubation for 5 min in a 37°C incubator in 1 ml of Cell Stripper (Mediatech Cellgro), and resuspended by addition of 3 ml of PBS per two wells. The cells were immediately fixed for 5 min in 4% paraformaldehyde prepared by addition of 1 ml of 16% paraformaldehyde (Electron Microscopy Sciences, Fort Washington, PA) to each 3-ml cell suspension. Fixed cells were pelleted and rinsed in 10 ml of PBS and pelleted again and resuspended in 0.25 ml of PBS and taken to the Rockefeller University Flow Cytometry Resource Center. EGFP and Alexa 633 emissions were collected simultaneously in a flow cytometer (FACSort, BD Biosciences, San Jose, CA) after gating with vector-transfected (pcDNA 3.1-) or single-color controls (Alexa Fluor 633-labeled Tf, EGFP, or AP180c-EGFP). In each experiment, 20,000 cells were analyzed per sample.

Calculation of fluorescence in static clathrin/epsin spots. A total of 35 static spots were identified from 3 cells. Clathrin spots were identified as static if they did not move laterally or if they did not move into the cell during the acquired image stream. The fluorescence in static clathrin/epsin spots was calculated as described previously for clathrin/AP-2 spots (30).

RESULTS

Evaluation of clathrin and AP-2 by time-lapse imaging. EGFP-tagged α -adaptin has previously been shown to be useful as a marker for AP-2: localization of the EGFP-tagged protein is indistinguishable from endogenous AP-2, and expression does not inhibit clathrin-mediated endocytosis (30, 32, 33, 45). In clathrin spots that remained static on the cell surface for a 30-s imaging period, the fluorescence intensity of EGFP- α -adaptin is similar to that of clathrin-DsRed. However, in the spots that disappeared at some point during the subsequent 30 s, the AP-2 fluorescence was over fivefold lower than in static spots (30, 33).

To assess whether there is a relation between the static spots that contained AP-2 and clathrin and the spots undergoing endocytosis that contained only clathrin, we imaged clathrin and AP-2 over longer periods of time. From 100-ms exposures every 500 ms for 5 min, we were able to image cells in rapid succession, so that individual events of internalization could be tracked reliably, while the total amount of time the cells could be evaluated without significant photobleaching was maximized.

Some of the observations of AP-2 over a 5-min period were indistinguishable from those over the shorter time periods. For example, AP-2 was not apparent in laterally mobile clathrin spots (data not shown). However, within 5 min, a number of EGFP- α -adaptin spots disappeared (Fig. 1, see supplemental Video 1 in the online version of this article). We then proceeded to investigate the behaviors associated with clathrin at these disappearing AP-2 spots.

Sites from which AP-2 fluorescence disappeared were identified, and clathrin-DsRed was present at every spot (89 disappearing AP-2 spots from 4 separate time-lapse sets; Fig. 1,

see supplemental Video 1). In 66% (59 of 89) of the cases in which AP-2 fluorescence decreased to background, clathrin fluorescence was subsequently observed to decrease to background before the end of the 5-min acquisition period. Examples of individual spots are shown in Fig. 1, in which AP-2 (Fig. 1A) and clathrin-DsRed (Fig. 1B) are quantitatively contrasted (Fig. 1C). Clathrin disappeared, on average, 26.2 ± 4.7 s later than AP-2, and a histogram of the delay in the decrease to background between AP-2 and clathrin is shown in Fig. 1D. In the remaining $\sim 34\%$ (30 of 89) of the events where AP-2 fluorescence decreased to background, clathrin remained in place, moved laterally, or fused with another clathrin spot but did not disappear. Thus the disappearance of AP-2 and clathrin from the cell surface is not tightly coupled in time (Fig. 1D). The largest single group in Fig. 1D reflects clathrin spots that did not disappear. Therefore, although the fluorescence of AP-2 and clathrin disappeared at the same location, the α -adaptin signal reached background much earlier than the clathrin signal.

We tested whether AP-2 fluorescence was disappearing sooner than clathrin fluorescence because of differences in the photochemical properties between EGFP and DsRed. Analyses identical to those described above were performed on cells coexpressing EGFP-clathrin and clathrin-DsRed, 5-min time lapses were imaged. The rates at which EGFP-clathrin and clathrin-DsRed spots disappeared were indistinguishable (23 spots from 3 cells, $P = 0.42$). The difference between the times of disappearance was 1.1 ± 1.3 s (with clathrin-DsRed disappearing before EGFP-clathrin), in contrast to 26.2 s between the disappearance of AP-2 and clathrin. This is consistent with the observation that other elements of endocytosis machinery attached to EGFP, e.g., dynamin-1 and dynamin-2 (33), and then disappeared from the cell surface with kinetics similar to those of clathrin-DsRed. Thus differences in photobleaching cannot account for the temporal disparity in the disappearance of AP-2 and clathrin.

If the fluorescence of AP-2 before disappearance were significantly closer to background than that of clathrin, it is possible that the apparent disassembly of AP-2 complexes before internalization of nascent CCVs could simply be a result of an inability to detect very low signal relative to background. Thus we compared fluorescence at the first frame for EGFP- α -adaptin spots that will later disappear with that for EGFP-clathrin spots in other cells ($n = 23$ spots from 3 cells per group). At the sites of internalization, the EGFP- α -adaptin fluorescence was 0.58 ± 0.05 , whereas the EGFP-clathrin fluorescence was 0.71 ± 0.10 ($P = 0.25$). Thus, although EGFP-clathrin did tend to be somewhat brighter relative to local background than EGFP- α -adaptin, the difference was not statistically significant and most likely would not account for the large difference in time of disappearance between clathrin and AP-2.

Epsin as a clathrin adaptor in forming CCVs. We next examined epsin, another molecule implicated as an adaptor, to test whether it, similar to AP-2, would dissociate before clathrin. To observe epsin simultaneously with clathrin during endocytosis, we used EGFP linked to the carboxy terminus of rat epsin 1 (epsin-EGFP) (42). Although this epsin-EGFP construct has previously been employed in live-cell TIR-FM imaging studies (42), we chose to confirm the utility of epsin-EGFP as a marker for plasma membrane-associated CCPs and

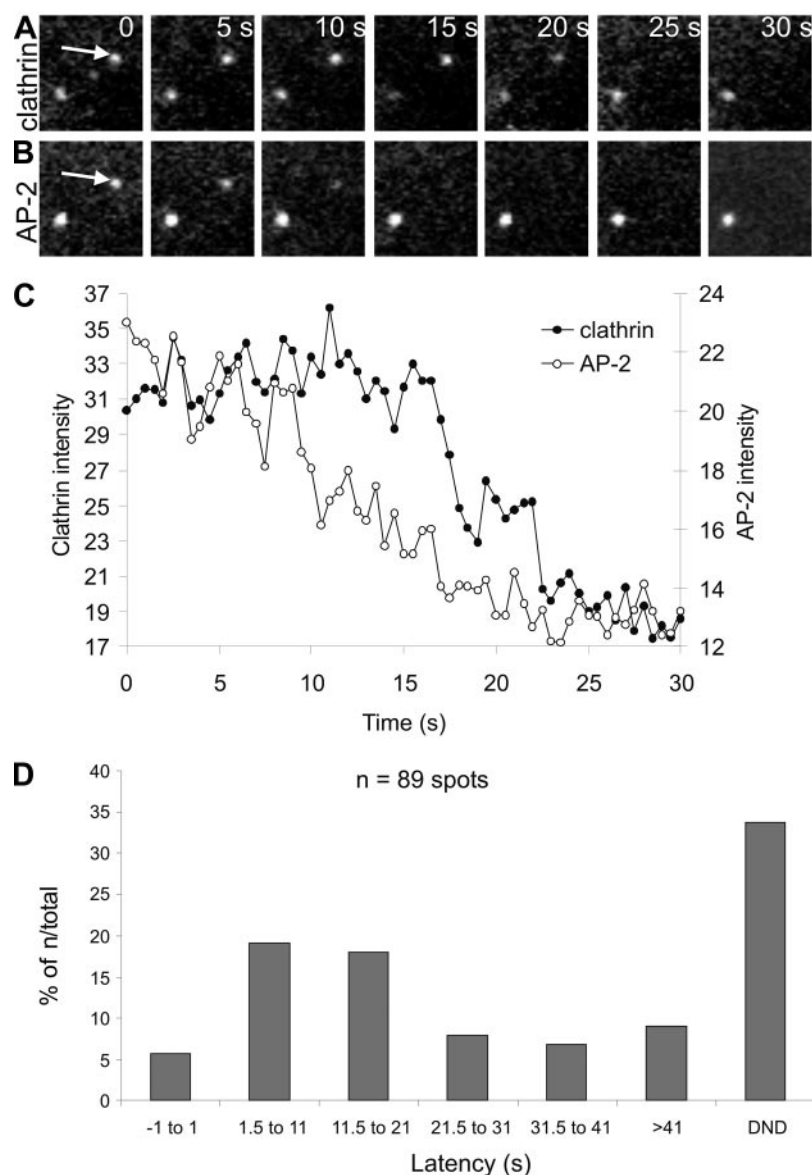


Fig. 1. Disappearance of adaptor complex-2 (AP-2) precedes that of clathrin. HeLa cells transfected with clathrin-DsRed (A) and enhanced green fluorescent protein (EGFP)-labeled α -adaptin (B) were imaged by total internal reflection fluorescence microscopy (TIR-FM). One frame (100-ms exposure time) every 5 s is presented from data acquired every 0.5 s for 5 min. Region represents a $3.84 \times 4.28 \mu\text{m}$ area. C: quantification of fluorescence intensity of the disappearing spot in A and B. D: analysis of clathrin spot dynamics at the sites of AP-2 disappearance. Difference between the time of disappearance of EGFP- α -adaptin and clathrin-DsRed is presented for 89 events of AP-2 disappearance from 4 time-lapse data sets. When clathrin remained in place, fused with another spot, or moved away laterally, the event is represented as "did not disappear" (DND).

CCVs. Epsin-EGFP colocalized with endogenous clathrin and cell surface TfR (Fig. 2). Quantification of these experiments determined that 97.2% (1,377 of 1,416 from 7 cells) of epsin-EGFP spots colocalized with clathrin, and 94% (1,387 of 1,475 from 7 cells) colocalized with TfR. These results suggest that epsin-EGFP localizes to CCPs and that expression of epsin-EGFP does not prevent the accumulation of endocytic cargo (TfR) at the sites of internalization, as observed when CCP/CCV formation is inhibited (5, 21). Further evidence in support of the proper localization of epsin-EGFP includes the observation that it colocalizes with other endogenous markers for CCPs, such as AP-2, CALM, and Eps-15 (see supplemental Fig. 1).

The effect of expression of epsin-EGFP was also checked with Tf uptake assayed by epifluorescence imaging. The results demonstrated that although expression of the dominant-negative AP180c-EGFP (12, 13) reduced Tf uptake, expression of epsin-EGFP did not (data not shown). There was no detectable effect on the internalization of Tf in cells expressing epsin-

EGFP on the basis of an analysis of >120 cells in each group (epsin-EGFP and AP180c-EGFP). However, there was considerable cell-to-cell variance in the amount of internalized Tf in these images. Therefore, the Tf uptake was quantified by flow cytometry, which verified that there was no deficiency in Tf internalization in cells expressing this epsin-EGFP (see supplemental Fig. 2). In contrast, expression of the dominant-negative control construct AP180c-EGFP (12, 13) clearly reduced Tf uptake into transfected cells evaluated in parallel (see supplemental Fig. 2).

Epsin-EGFP localized to CCPs when TIR-FM was used to image fluorescence at the cell surface (Fig. 3); 100% (400 of 400 from 4 data sets) of epsin-EGFP spots colocalized with clathrin-DsRed, and 96.8% (387 of 400 from 4 data sets) of clathrin-DsRed spots colocalized with epsin-EGFP. In previous studies, we found that in static spots the fluorescence of clathrin-DsRed was equal to that of EGFP- α -adaptin (30, 33). In contrast, there was considerably greater background fluorescence in the epsin-EGFP images (Fig. 3B). As a result, the

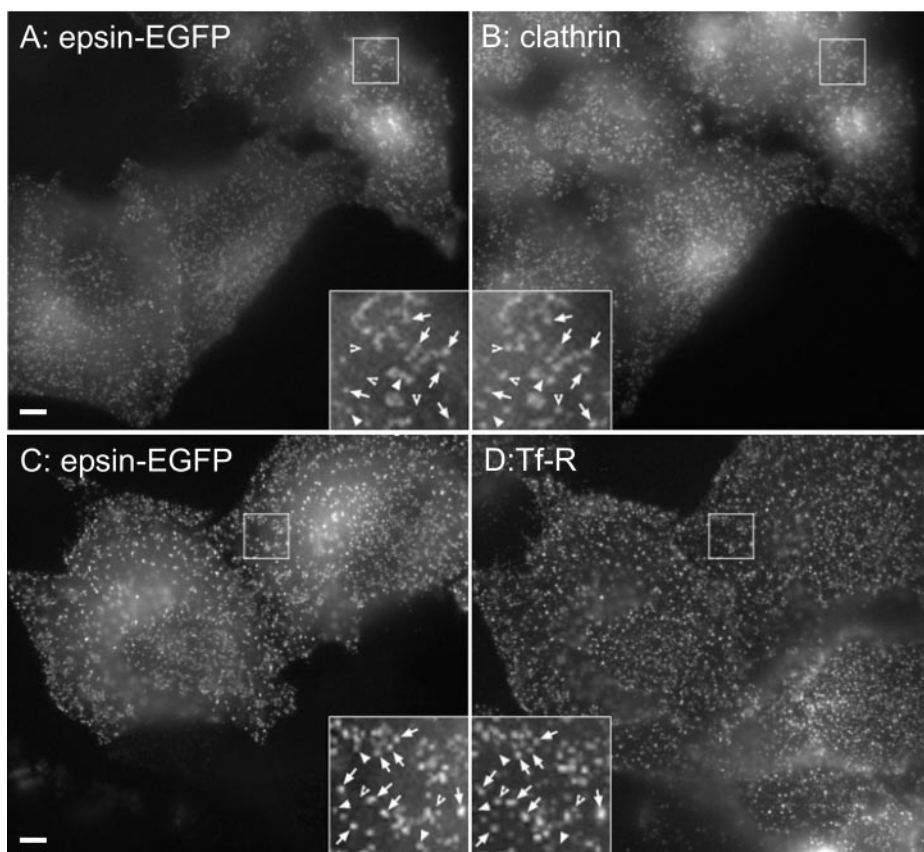


Fig. 2. Colocalization of epsin-EGFP and endogenous markers of clathrin-coated pits. Transfected HeLa cells expressing epsin-EGFP were immunolabeled for endogenous clathrin or transferrin receptor (TfR). Arrows, colocalized puncta; arrowheads, epsin-EGFP puncta devoid of clathrin (B) or TfR (D); partial arrowheads, clathrin (B) and TfR (D) spots negative for epsin-EGFP. Scale bar, 5 μ m.

epsin-EGFP was 0.18 ± 0.02 above background, whereas clathrin was 1.07 ± 0.27 above background (35 static spots from 3 cells, $P = 0.0018$). The high background of the epsin limited the types of experimental evaluations and quantitative studies that can be performed with epsin-EGFP.

When cells expressing clathrin-DsRed and epsin-EGFP were assayed for colocalization in disappearing spots, 65.7% (46 of 70 from 6 image stacks) of clathrin spots that subsequently internalized into the cell colocalized with epsin-EGFP in the first frame. In contrast, only 3.3% (2 of 60 from 4 image

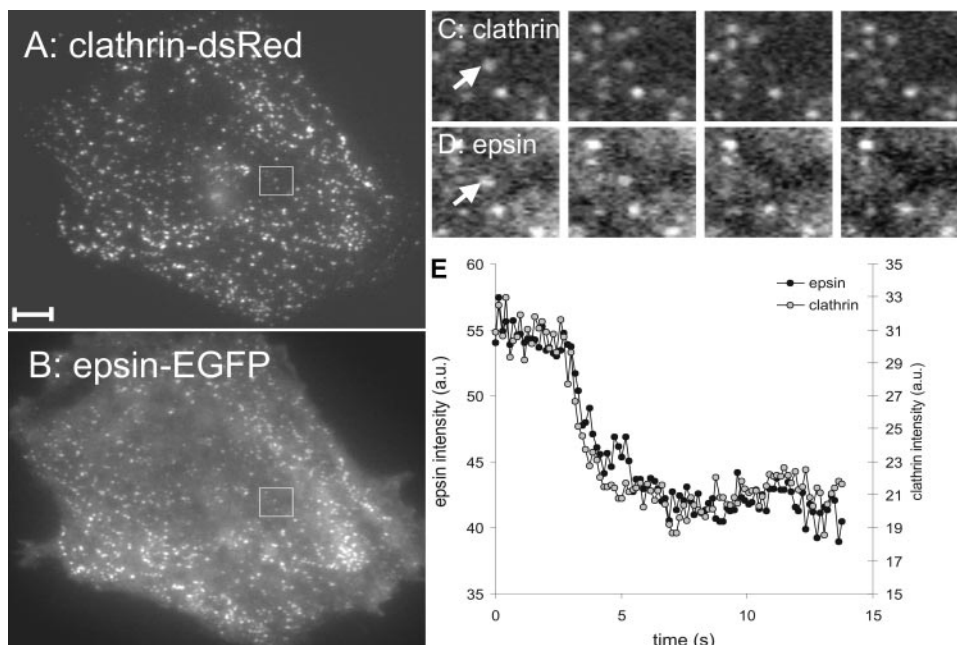


Fig. 3. Colocalization of epsin-EGFP and clathrin-DsRed in disappearing spots. A and B: HeLa cells cotransfected with clathrin-DsRed and epsin-EGFP were imaged by TIR-FM. Scale bar, 5 μ m. C and D: images from video acquired at 240 ms per frame and shown every 15 frames demonstrating simultaneous disappearance of clathrin and epsin. E: quantification of fluorescence intensity of disappearing puncta shown in supplemental Video 2 (see online supplement). au, Arbitrary units.

stacks) of laterally mobile clathrin-DsRed spots colocalized with epsin-EGFP. Furthermore, when individual disappearing clathrin/epsin spots were evaluated over time, the clathrin-DsRed and epsin-EGFP disappeared from the cell surface at the same location, time, and rate (see supplemental Video 2). The results were indistinguishable, whether the data were analyzed by direct fluorescence quantification (Fig. 3) or by line-scan analysis (Fig. 4). This is in contrast to the observation that the AP-2 complex is largely absent from disappearing spots relative to the static population (30, 33).

Characterization of static clathrin spots over time. Over short (e.g., 1-min) periods, fluorescent-tagged clathrin has been observed to exist in active and static populations at the cell surface (14, 25, 30, 32, 33, 46). Indeed, we previously saw that only ~15% of clathrin puncta internalize over a 1-min period (31). To determine whether static clathrin spots represent sites of future endocytosis or an independent population that may never internalize, we analyzed the dynamics of clathrin over longer time periods. Cells expressing clathrin-DsRed were imaged for 10 min, with 100-ms exposures acquired every 1 s, producing a time-lapse series of 600 frames. When images from the same region were analyzed every 2 min, some static spots persisted for the entire 10-min time period; within the region shown in Fig. 5, ~33% (9 of 27) of the spots remained after 10 min.

To further elucidate static clathrin spots, the behavior of clathrin at the surface was quantified over a 30-min period (100 ms acquired every 6 s). Because of the longer imaging time in these studies, it was essential to track each individual spot of interest to avoid miscategorization due to local spot motion or overall motion of the cell. In these studies, 200 spots per time lapse from a total of 5 separate data sets were tracked (a total of 1,000 spots). A majority (about two-thirds) of the spots were lost from the static population during the initial 10 min, i.e., disappeared, moved laterally in the plane of the membrane, or fused with another spot (Fig. 6A, see supplemental Video 3), whereas 22% remained static for the entire 30 min. For the spots that were present on the surface at *time 0*, the highest rate of decrease occurred during the initial 10 min. The rate of internalization of these initial spots slowed considerably during each subsequent 10-min period. The absolute number of static spots remaining at each time point varied from region to region. However, the general trend was consistent: there was a rapid loss of a majority of spots during the first 10-min period, and the remaining spots were static during each subsequent 10-min period.

The quantitative analysis was repeated with a focus on events within the first 10-min time period. Fifty spots per region (250 spots total) that were known to become active between 0 and 10 min were randomly selected and tracked.

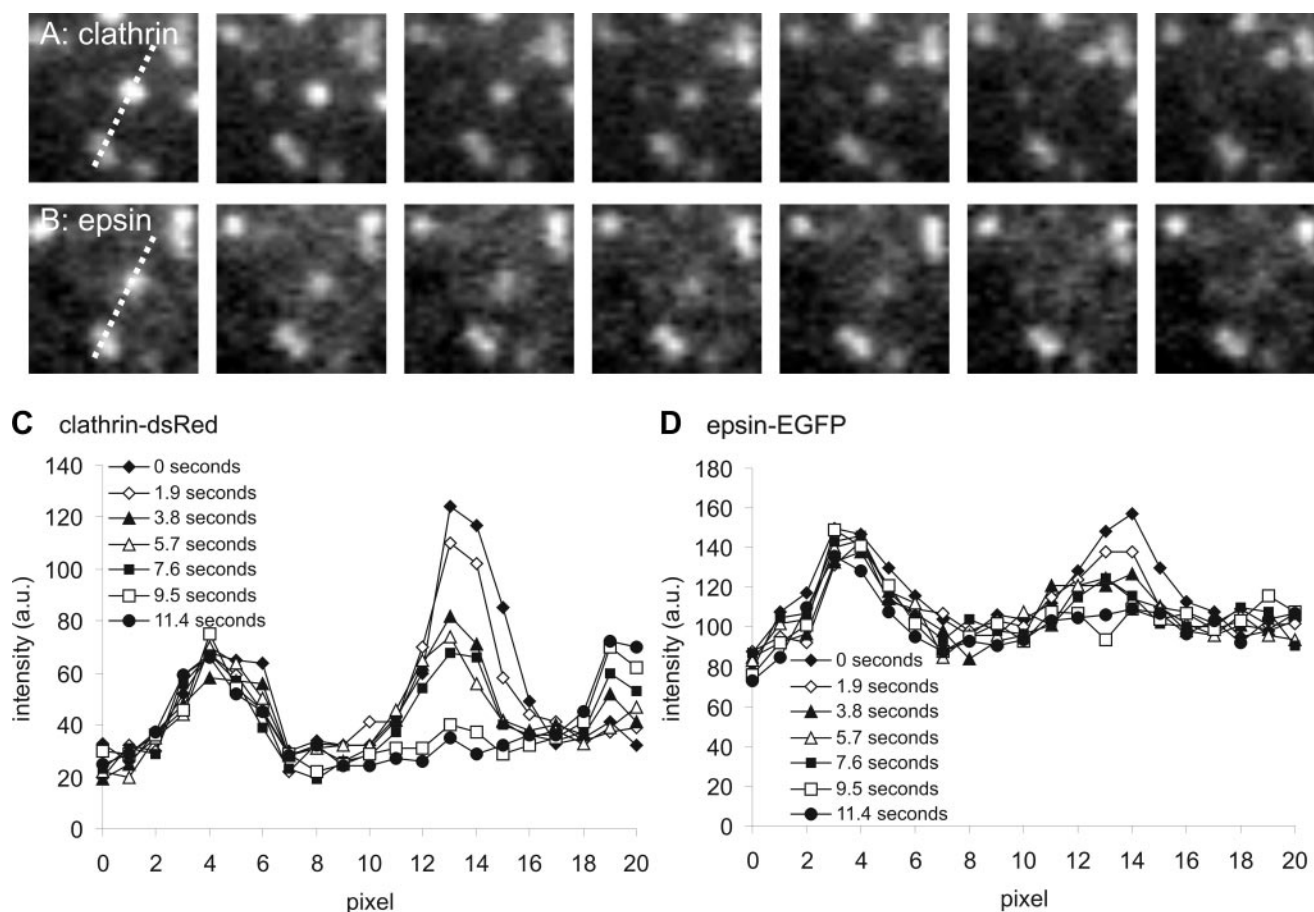
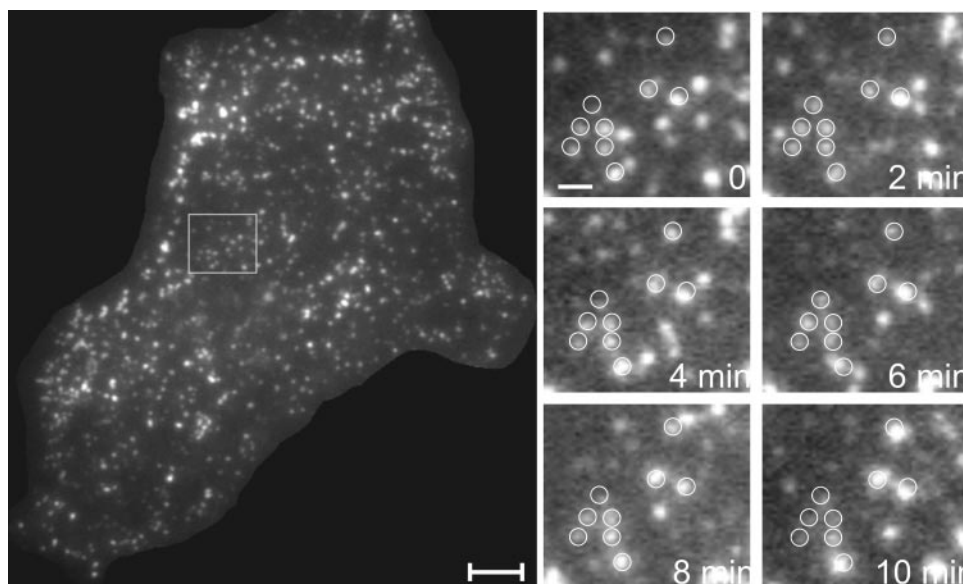


Fig. 4. Line-scan analysis of epsin-EGFP and clathrin-DsRed in disappearing and static spots. *A* and *B*: HeLa cells cotransfected with clathrin-DsRed and epsin-EGFP were imaged by TIR-FM and quantified with a line scan (21×1 pixel, 108 nm per pixel) along the region marked by dashed lines. *C* and *D*: line-scan quantification of clathrin-DsRed and epsin-EGFP and analysis of images in *A* and *B* at 10-frame intervals from a video acquired at 190 ms per frame.

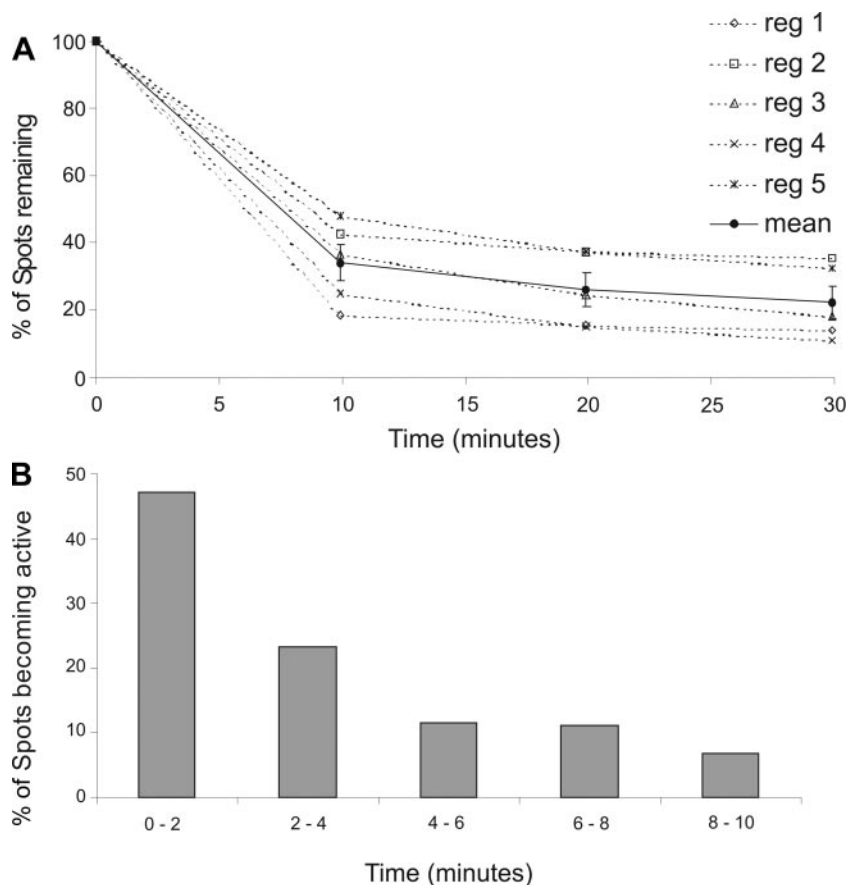
Fig. 5. Static clathrin spots (encircled) remain in place for ≥ 10 min (right), as shown in time-lapse TIR-FM of HeLa cells expressing clathrin-DsRed acquired at 1-s intervals (left). Scale bar, 5 μ m.



The results of this analysis are presented in Fig. 6B. Although spots became active throughout the entire 10 min, the majority of these events occurred at the beginning of the time interval, 70% during the first 4 min. These results (Figs. 5 and 6) indicate that a population of static spots remain at the cell surface for long (≥ 30 -min) periods and that those spots destined to become active will do so relatively rapidly.

These results could be explained by two different hypotheses. 1) The clathrin spots fall into two groups: one with a 70% probability of internalizing within 4 min and another that internalizes at a significantly slower rate, if at all. 2) During the imaging period, the net rate of endocytosis may be slowing. To distinguish between these hypotheses, 200 new spots were identified at the 10-min time point for one of the regions

Fig. 6. Time course of clathrin spot disappearance. A: average number of clathrin spots remaining at 0, 10, 20, and 30 min. Values are means \pm SE ($n = 1,000$ spots, 200 spots per region for 5 separate time lapses). One frame (100-ms exposure time) was acquired every 6 s for 30 min. A: percent remaining at each time point for each region (reg). B: time at which clathrin puncta that moved or disappeared during the first 10 min became active ($n = 50$ active spots per region for 5 regions).



presented in Fig. 6 (*region 5*). Inasmuch as the percentage of spots remaining at the end of the 10- to 20-min imaging interval was similar to that between 0 and 10 min for this same region (both $\sim 50\%$), the total rate of endocytosis is not slowing during the period of imaging.

We tested whether clathrin in the static spots exchanges with cytosolic subunits. This exchange is lost on gross inhibition of endocytosis by manipulations such as potassium depletion and hypertonic sucrose treatment (23, 44, 45). When the static population of clathrin spots was subjected to FRAP, 89 static clathrin spots were identified in 10-min time-lapse data sets. Subsequent to photobleaching, recovery was tracked over a second 10-min time lapse (Fig. 7). The static photobleached clathrin spots recovered with a $t_{1/2}$ of 163.8 ± 10.3 s.

DISCUSSION

Clathrin-mediated endocytosis requires the coordination of a number of proteins to control cargo clustering and sorting, clathrin coat formation, induction and maintenance of membrane curvature, and fission of the nascent vesicle (8, 35, 36). In addition to cargo and clathrin, this process involves clathrin-associated cargo adaptors and accessory proteins, as well as specific phospholipids and cytoskeletal elements (9, 11, 41).

Our previous studies evaluated the behaviors associated with many examples from these categories, including clathrin, Tf, dynamin-1 and dynamin-2, and markers for the AP-2 complex (α - and β -adaptin) (30, 32–34). These investigations provided information that requires an elaboration on most current models (32). For example, clathrin at the cell surface is not a homogenous population but, rather, exists as spots; some of these spots are static, some move laterally parallel to the membrane, and some move into the cell, perpendicular to the surface (18, 26, 30, 32, 33, 46). The adaptor complex AP-2 is present in the static spots (CCPs) but is excluded from spots undergoing internalization (CCVs) (30, 33). This present work

contrasts these observations with those of another clathrin adaptor, epsin, and expands these studies by addressing the relations between these different populations of clathrin puncta.

Evaluation of clathrin and AP-2 by time-lapse imaging. Clathrin and AP-2 colocalize within the majority of spots at the cell surface, and the fluorescence intensity of clathrin-DsRed and EGFP- α -adaptin within static spots is equal (30, 33). Yet, in clathrin-coated structures that will internalize over the subsequent 30 s, the fluorescence of AP-2 is usually indistinguishable from background. These observations could be explained by at least three hypotheses: 1) CCVs can be produced and internalize with no contribution from AP-2; 2) AP-2-negative CCVs can iteratively bud from AP-2-positive clathrin spots (CCPs), potentially sites of cargo sorting; and 3) AP-2 is released from the nascent vesicle before internalization. Evidence in support of *hypothesis 1* includes the observation that endocytosis of certain ligands persists after silencing of α -adaptin expression. This is consistent with certain CCVs forming in the absence of AP-2 (16, 27). *Hypothesis 2* suggests an iterative budding of nascent CCVs from static sites, which is consistent with our observations and those of others (26, 46). Furthermore, we previously observed the separation and subsequent disappearance of clathrin spots from static spots containing clathrin and AP-2 (30). *Hypothesis 3*, that AP-2 can leave endocytic coats while leaving clathrin behind, is supported by the present (Fig. 1), as well as earlier (15, 30), observations. Thus there is heterogeneity in the population of clathrin at the surface (in terms of static or mobile status) and heterogeneity in the behaviors with which AP-2 and clathrin separate from one another. Studies of single events are powerful tools for understanding a molecular mechanism, and our observations draw attention to the importance of studying many events and archiving the diversity of behaviors.

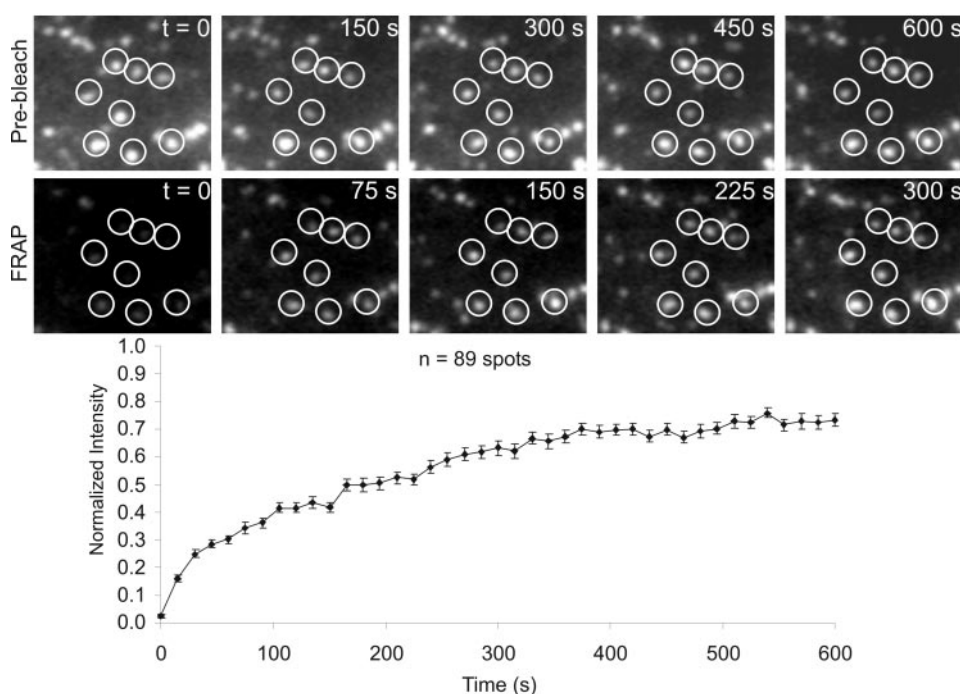


Fig. 7. Fluorescence recovery after photobleaching (FRAP) analysis of 89 static clathrin spots. Static spots were identified from dynamics of clathrin puncta during the first 10 min of image acquisition (prebleach). After 1 min of exposure to bleach, fluorescence recovery was measured for 10 min in the corresponding encircled regions, averaged, and plotted.

It is possible that AP-2 fluorescence disappeared before clathrin fluorescence because adaptor proteins segregated to the pole of nascent CCVs farthest from the membrane before membrane fission. This possibility, which we raised previously (33), has not been disproved. However, because our penetration depth is greater than the diameter of a CCV (22), this is probably not the case. Furthermore, inasmuch as epsin and clathrin disappeared simultaneously (Figs. 3 and 4), this could not be true for all clathrin adaptors.

During our analysis of clathrin and AP-2 time-lapse data, we occasionally observed an apparent partial dimming of clathrin during the disappearance of AP-2 (data not shown). The iterative vertical disappearance of portions of clathrin spots (without prior lateral motion away from the residual static puncta) is not a behavior that we previously characterized, and it is difficult to distinguish between this possibility and the potential effects of photobleaching, particularly when only 100 ms are imaged every 500 ms. Thus, although it is possible that multiple nascent CCVs can internalize without any lateral movement, we have avoided overinterpretation of this apparent finding. However, we cannot exclude the possibility that, in some cases, AP-2 and a portion of a spot's total clathrin complement can disappear together before internalization of the residual clathrin. If this does occur, it could represent any one of several events: 1) disengagement of all AP-2 and some clathrin before coated vesicle internalization, 2) retraction of AP-2 and/or clathrin from the membrane before fission, or 3) AP-2-positive CCV (an unlikely, but nonetheless possible, occurrence).

Evaluation of epsin-EGFP during clathrin-mediated endocytosis. Our preliminary observations demonstrate that epsin-EGFP is a useful probe for continuous imaging of clathrin-mediated endocytosis by TIR-FM. It localizes to CCPs marked by endogenous endocytic proteins, and expression does not impede the process of clathrin-mediated endocytosis (Fig. 2, see supplemental Figs. 1 and 2). When clathrin-DsRed and epsin-EGFP are imaged simultaneously, epsin is found in nearly all (96.8%) clathrin spots but is not detectable in the small population of the laterally mobile clathrin spots that have been previously shown to move along the microtubule cytoskeleton (34) and are devoid of AP-2 (33).

Previous biochemical analyses have been unable to unambiguously assign epsin a place within or without the nascent CCV (6, 7, 28, 29). The majority (65.7%) of the clathrin spots that disappeared from the surface contain epsin, which disappeared at the same site, time, and rate as clathrin (Figs. 3 and 4, see supplemental Video 2), whereas in the remaining ~33% of disappearing clathrin-DsRed spots, epsin-EGFP was not detected above background. This observation provides strong evidence for the presence of epsin in these CCVs. Although the simultaneous disappearance of epsin-EGFP and clathrin-DsRed does not prove that epsin is retained as part of the nascent CCV, because the penetration depth is greater than the diameter of a CCV (22), we would most likely have observed whether epsin was lost before fission or internalization. Thus the observation that epsin remains with clathrin differs from the observation that AP-2 was absent from the laterally mobile and disappearing populations of clathrin (30, 33). This raises the possibility that epsin may replace AP-2 as the clathrin adaptor in formation of CCVs, although there may be other potential functional roles for epsin during endocytosis.

Characterization of static clathrin spots over time. In our previous analyses, during <1-min image streams, the majority of clathrin spots on the cell surface were static: they neither disappeared nor moved laterally in the plane of the plasma membrane (33). We tested for a relation between the static and dynamic populations of clathrin spots by imaging for longer periods of time. The results demonstrate that even the clathrin spots that were static for the 30-s observation period are a heterogeneous population. A minority (22%) remained static throughout a 30-min period (Fig. 6). The majority of the remaining spots disappeared within the first 4 min. The observation that a proportion of clathrin at the cell surface remains static for very long periods could be consistent with the hypothesis that there is an "aging process" for clathrin, in which newly synthesized clathrin is more efficacious in endocytosis (10, 17). This has been posited to be the result of alterations in the regulation by heat shock cognate-70 or older clathrin becoming trapped in nonfunctional coated pits.

These longer-term static puncta retain some of the phenotype of "active" clathrin. When they are photobleached, they are observed to recover with $t_{1/2}$ of 163.8 ± 10.3 s. The ability to exchange with cytosolic clathrin differs from the complete block of subunit exchange observed when clathrin-mediated endocytosis is blocked by hypertonic sucrose or potassium depletion. Thus even the "static" clathrin may be contributing in a yet-to-be-defined manner to clathrin-mediated endocytosis.

ACKNOWLEDGMENTS

The authors thank Dr. Marina Fix for assistance in the preparation of the manuscript and Dr. Svetlana Mazel (Rockefeller University Flow Cytometry Resource Center) for assistance with the fluorescence-activated cell sorter experiments.

GRANTS

This work was supported by National Institute of General Medical Sciences Grant 1 F32 GM-069200-03 (J. Z. Rappoport), Association pour la Recherche contre le Cancer Grant 36-91 (A. Benmerah), and National Science Foundation Grants BES-0620813 and BES-0322867 (S. M. Simon).

REFERENCES

1. Axelrod D. Total internal reflection fluorescence microscopy in cell biology. *Traffic* 2: 764–774, 2001.
2. Benmerah A, Bayrou M, Cerf-Bensussan N, and Dautry-Varsat A. Inhibition of clathrin-coated pit assembly by an Eps15 mutant. *J Cell Sci* 112: 1303–1311, 1999.
3. Benmerah A, Begue B, Dautry-Varsat A, and Cerf-Bensussan N. The ear of α -adaptin interacts with the COOH-terminal domain of the Eps 15 protein. *J Biol Chem* 271: 12111–12116, 1996.
4. Benmerah A, Lamaze C, Begue B, Schmid SL, Dautry-Varsat A, and Cerf-Bensussan N. AP-2/Eps15 interaction is required for receptor-mediated endocytosis. *J Cell Biol* 140: 1055–1062, 1998.
5. Benmerah A, Poupon V, Cerf-Bensussan N, and Dautry-Varsat A. Mapping of Eps15 domains involved in its targeting to clathrin-coated pits. *J Biol Chem* 275: 3288–3295, 2000.
6. Blondeau F, Ritter B, Allaire PD, Wasiaak S, Girard M, Hussain NK, Angers A, Legendre-Guillemain V, Roy L, Boismenu D, Kearney RE, Bell AW, Bergeron JJ, and McPherson PS. Tandem MS analysis of brain clathrin-coated vesicles reveals their critical involvement in synaptic vesicle recycling. *Proc Natl Acad Sci USA* 101: 3833–3838, 2004.
7. Chen H, Fre S, Slepnev VI, Capua MR, Takei K, Butler MH, Di Fiore PP, and De Camilli P. Epsin is an EH-domain-binding protein implicated in clathrin-mediated endocytosis. *Nature* 394: 793–797, 1998.
8. Conner SD and Schmid SL. Regulated portals of entry into the cell. *Nature* 422: 37–44, 2003.

9. **De Camilli P, Chen H, Hyman J, Panepucci E, Bateman A, and Brunger AT.** The ENTH domain. *FEBS Lett* 513: 11–18, 2002.
10. **Di Paolo G and De Camilli P.** Does clathrin pull the fission trigger? *Proc Natl Acad Sci USA* 100: 4981–4983, 2003.
11. **Engqvist-Goldstein AE and Drubin DG.** Actin assembly and endocytosis: from yeast to mammals. *Annu Rev Cell Dev Biol* 19: 287–332, 2003.
12. **Ford MG, Mills IG, Peter BJ, Vallis Y, Praefcke GJ, Evans PR, and McMahon HT.** Curvature of clathrin-coated pits driven by epsin. *Nature* 419: 361–366, 2002.
13. **Ford MG, Pearce BM, Higgins MK, Vallis Y, Owen DJ, Gibson A, Hopkins CR, Evans PR, and McMahon HT.** Simultaneous binding of PtdIns(4,5)P₂ and clathrin by AP180 in the nucleation of clathrin lattices on membranes. *Science* 291: 1051–1055, 2001.
14. **Gaidarov I, Santini F, Warren RA, and Keen JH.** Spatial control of coated-pit dynamics in living cells. *Nat Cell Biol* 1: 1–7, 1999.
15. **Hannan LA, Newmyer SL, and Schmid SL.** ATP- and cytosol-dependent release of adaptor proteins from clathrin-coated vesicles: a dual role for Hsc70. *Mol Biol Cell* 9: 2217–2229, 1998.
16. **Hinrichsen L, Harborth J, Andrees L, Weber K, and Ungewickell EJ.** Effect of clathrin heavy chain- and α -adaptin-specific small inhibitory RNAs on endocytic accessory proteins and receptor trafficking in HeLa cells. *J Biol Chem* 278: 45160–45170, 2003.
17. **Iversen TG, Skretting G, van Deurs B, and Sandvig K.** Clathrin-coated pits with long, dynamin-wrapped necks upon expression of a clathrin antisense RNA. *Proc Natl Acad Sci USA* 100: 5175–5180, 2003.
18. **Keyel PA, Watkins SC, and Traub LM.** Endocytic adaptor molecules reveal an endosomal population of clathrin by total internal reflection fluorescence microscopy. *J Biol Chem* 279: 13190–13204, 2004.
19. **Kirchhausen T.** Clathrin adaptors really adapt. *Cell* 109: 413–416, 2002.
20. **Kusner L and Carlin C.** Potential role for a novel AP180-related protein during endocytosis in MDCK cells. *Am J Physiol Cell Physiol* 285: C995–C1008, 2003.
21. **Lamaze C, Fujimoto LM, Yin HL, and Schmid SL.** The actin cytoskeleton is required for receptor-mediated endocytosis in mammalian cells. *J Biol Chem* 272: 20332–20335, 1997.
22. **Lampson MA, Schmoranzler J, Zeigerer A, Simon SM, and McGraw TE.** Insulin-regulated release from the endosomal recycling compartment is regulated by budding of specialized vesicles. *Mol Biol Cell* 12: 3489–3501, 2001.
23. **Loerke D, Wienisch M, Kochubey O, and Klingauf J.** Differential control of clathrin subunit dynamics measured with EW-FRAP microscopy. *Traffic* 6: 918–929, 2005.
24. **Loerke D, Wienisch M, Kochubey O, and Klingauf J.** Differential control of clathrin subunit dynamics measured with EW-FRAP microscopy. *Traffic* 6: 918–929, 2005.
25. **Merrifield CJ, Feldman ME, Wan L, and Almers W.** Imaging actin and dynamin recruitment during invagination of single clathrin-coated pits. *Nat Cell Biol* 4: 691–698, 2002.
26. **Merrifield CJ, Perrais D, and Zenisek D.** Coupling between clathrin-coated pit invagination, cortactin recruitment, and membrane scission observed in live cells. *Cell* 121: 593–606, 2005.
27. **Motley A, Bright NA, Seaman MN, and Robinson MS.** Clathrin-mediated endocytosis in AP-2-depleted cells. *J Cell Biol* 162: 909–918, 2003.
28. **Mousavi SA, Malerod L, Berg T, and Kjekens R.** Clathrin-dependent endocytosis. *Biochem J* 377: 1–16, 2004.
29. **Nossal R and Zimmerberg J.** Endocytosis: curvature to the ENTH degree. *Curr Biol* 12: R770–R772, 2002.
30. **Rappoport JZ, Benmerah A, and Simon SM.** Analysis of the AP-2 adaptor complex and cargo during clathrin-mediated endocytosis. *Traffic* 6: 539–547, 2005.
31. **Rappoport JZ and Simon SM.** Real-time analysis of clathrin-mediated endocytosis during cell migration. *J Cell Sci* 116: 847–855, 2003. [Corrigenda. *J Cell Sci* 116: 15 March 2003, p. 1151.]
32. **Rappoport JZ, Simon SM, and Benmerah A.** Understanding living clathrin-coated pits. *Traffic* 5: 327–337, 2004.
33. **Rappoport JZ, Taha BW, Lemeer S, Benmerah A, and Simon SM.** The AP-2 complex is excluded from the dynamic population of plasma membrane-associated clathrin. *J Biol Chem* 278: 47357–47360, 2003.
34. **Rappoport JZ, Taha BW, and Simon SM.** Movement of plasma-membrane-associated clathrin spots along the microtubule cytoskeleton. *Traffic* 4: 460–467, 2003.
35. **Robinson MS.** The role of clathrin, adaptors and dynamin in endocytosis. *Curr Opin Cell Biol* 6: 538–544, 1994.
36. **Schmid SL.** Clathrin-coated vesicle formation and protein sorting: an integrated process. *Annu Rev Biochem* 66: 511–548, 1997.
37. **Schmid SL, McNiven MA, and De Camilli P.** Dynamin and its partners: a progress report. *Curr Opin Cell Biol* 10: 504–512, 1998.
38. **Schmoranzler J, Goulian M, Axelrod D, and Simon SM.** Imaging constitutive exocytosis with total internal reflection fluorescence microscopy. *J Cell Biol* 149: 23–32, 2000.
39. **Song BD, Yarar D, and Schmid SL.** An assembly-incompetent mutant establishes a requirement for dynamin self-assembly in clathrin-mediated endocytosis in vivo. *Mol Biol Cell* 15: 2243–2252, 2004.
40. **Takei K and Haucke V.** Clathrin-mediated endocytosis: membrane factors pull the trigger. *Trends Cell Biol* 11: 385–391, 2001.
41. **Traub LM.** Sorting it out: AP-2 and alternate clathrin adaptors in endocytic cargo selection. *J Cell Biol* 163: 203–208, 2003.
42. **Tsuboi T, McMahon HT, and Rutter GA.** Mechanisms of dense core vesicle recapture following “kiss and run” (“cavicapture”) exocytosis in insulin-secreting cells. *J Biol Chem* 279: 47115–47124, 2004.
43. **Wendland B.** Epsins: adaptors in endocytosis? *Nat Rev Mol Cell Biol* 3: 971–977, 2002.
44. **Wu X, Zhao X, Baylor L, Kaushal S, Eisenberg E, and Greene LE.** Clathrin exchange during clathrin-mediated endocytosis. *J Cell Biol* 155: 291–300, 2001.
45. **Wu X, Zhao X, Puertollano R, Bonifacino JS, Eisenberg E, and Greene LE.** Adaptor and clathrin exchange at the plasma membrane and trans-Golgi network. *Mol Biol Cell* 14: 516–528, 2003.
46. **Yarar D, Waterman-Storer CM, and Schmid SL.** A dynamic actin cytoskeleton functions at multiple stages of clathrin-mediated endocytosis. *Mol Biol Cell* 16: 964–975, 2005.